ORGANOMETALLICS

pubs.acs.org/Organometallics Article

Catalytic C−H Bond Alkylation of Azoles with Alkyl Halides Mediated by Nickel(II) Complexes of Phenanthridine-Based *N*^*N*⁻^*N* Pincer Ligands

Pavan Mandapati, Jason D. Braun, Baldeep K. Sidhu, Gabrielle Wilson, and David E. Herbert*

Cite This: https://dx.doi.org/10.1021/acs.organomet.0c00161 Read Online

ACCESS | Metrics & More | Article Recommendations | Supporting Information

ABSTRACT: Ni(II) complexes supported by tridentate *N*^*N*⁻^*N* diarylamido pincer-type ligands have been demonstrated to act as active catalysts in the carbon−carbon bond forming alkylation of azoles using unactivated alkyl halides. Here, we show that benzannulated phenanthridine-containing ligands can form homogeneous Ni(II) catalysts active with both benzoxazole and benzothiazole substrates. These precatalysts have been fully characterized in solution and the solid state, including by cyclic voltammetry.

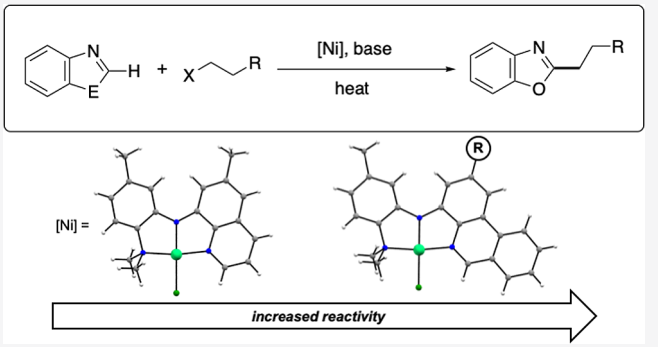

INTRODUCTION

The homogeneous catalytic conversion of C−H bonds to C−C bonds mediated by coordination complexes of first-row transition metals is of prime interest in the drive to increase sustainability in chemical synthesis.[1,2] First, direct functionalization of C−H bonds obviates the need for leaving groups that can limit atom economy.[3] Second, the use of first-row metal catalysts reduces reliance on less abundant precious metals for transformations that add value to organic substrates such as aromatic heterocycles.[4] With respect to these widely used synthetic building blocks, transition metal catalyzed C−H alkylation reactions using alkyl halides with β-hydrogens can be challenging, as β-hydride elimination can lead to unproductive side reactions.[5] As a result, a relatively limited number of examples of such cross-couplings have been reported, with palladium,[6,7] nickel,[8−11] and copper[12−14] catalysts featuring most prominently.

Well-defined complexes of nickel supported by diarylamido *N*^*N*⁻^*N* pincer-type ligands, in particular, have been shown to direct the alkylation of oxazoles and thiazoles using unactivated alkyl halides (Figure 1).[8,10] While Ni(II) complexes of bis(2-(dimethylamino)phenyl)amido ligands (**A**) show excellent catalytic activity, as reported by Hu and co-workers, addition of a copper cocatalyst is necessary to achieve high yields.[8] Moreover, decomposition of **A** was observed over time under the high temperature reaction conditions, depositing nanoparticulate metal into the reaction mixture.[8] Punji and co-workers elaborated this scaffold into a more robust quinolinyl-based pincer type analogue. The corresponding Ni chloride complexes supported by a (2-(dimethylamino)phenyl)(8-quinolinyl)amido donor set (**B**) exhibit greater temperature stability and do not require a cocatalyst in the catalytic alkylation of benzothiazoles.[10]

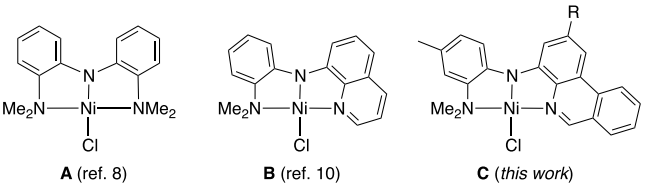

Figure 1. *N*^*N*⁻^*N* pincer-type ligand supported Ni complexes for the C−H alkylation of azoles (**A**, see ref 8; **B**, see ref 10; **C**, this work).

We recently described synthetic routes to tridentate, *N*^*N*⁻^*N* diarylamido pincer-type ligands bearing benzannulated phenanthridine (3,4-benzoquinoline) heterocyclic donor arms.[15] Compared with (8-amino)quinolines, a relatively broad range of 2-substituted (4-amino)phenanthridines can be easily accessed via tandem cross-coupling/condensation reactions using various 4-substituted anilines;[16] accessing 6-substituted (8-amino)quinolines can require less tractable Skraup reaction conditions.[17] Moreover, in these benzannulated pincer-type frameworks, the phenanthridinyl donor arm

Received: March 5, 2020

Scheme 1. Synthesis of (a) Phenanthridine Precursors, (b) Phenanthridine-Based *N^N(H)^N* Proligands and Nickel Complexes, and (c) Methyl-Substituted Quinolinyl Analogues of B,[10] Described in This Work

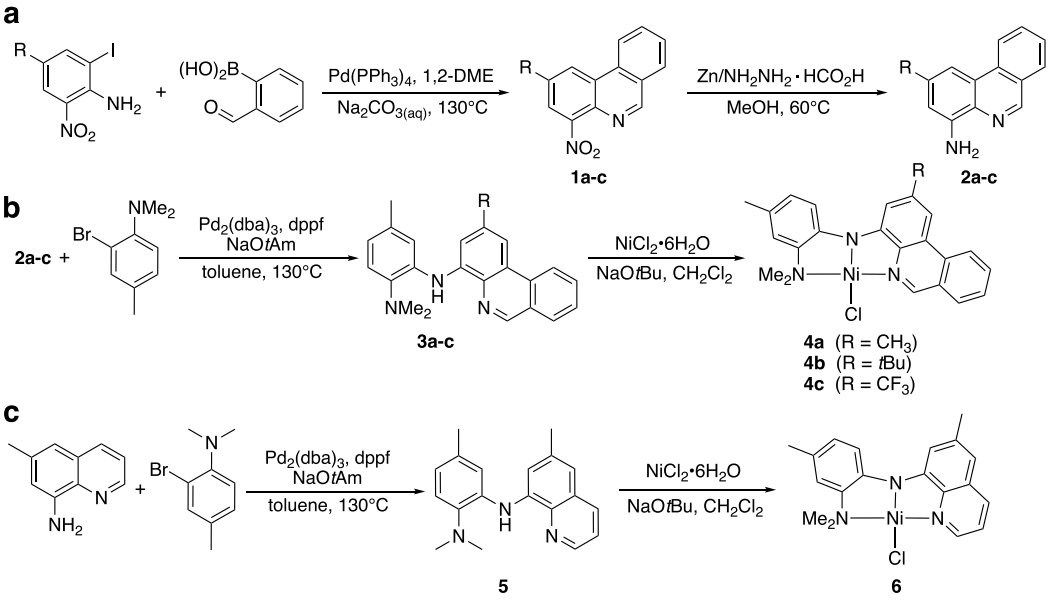

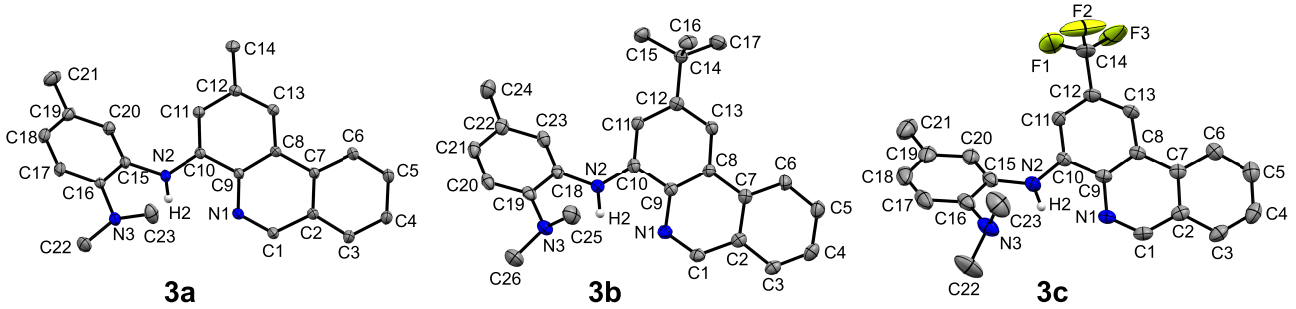

Figure 2. Solid-state structures of **3a−c** shown with thermal ellipsoids at 50% probability levels. Hydrogens other than H2 are omitted for clarity. Selected bond distances (Å) and angles (deg) for **3a**: C(1)−N(1) 1.3034(11), C(10)−N(2) 1.3957(10), C(15)−N(2) 1.4124(11), C(16)−N(3) 1.4168(12); C(10)−N(2)−C(15) 122.64(7), C(9)−C(10)−N(2) 117.25(7), C(16)−C(15)−N(2) 121.17(8). **3b**: C(1)−N(1) 1.302(3), C(10)−N(2) 1.386(3), C(18)−N(2) 1.397(3), C(23)−N(3) 1.425(3); C(10)−N(2)−C(18) 128.8(2), C(9)−C(10)−N(2) 115.4(2), C(19)−C(18)−N(2) 122.4(2). **3c**: C(1)−N(1) 1.291(4), C(10)−N(2) 1.374(3), C(15)−N(2) 1.395(4), C(16)−N(3) 1.430(4); C(10)−N(2)−C(15) 129.9(2), C(9)−C(10)−N(2) 116.2(2), C(16)−C(15)−N(2) 116.6(3).

can act as an efficient Lewis base with strong π-acid character thanks to the presence of low-lying vacant orbitals[18] and are sterically less encumbered than isomeric acridines.[19] As mechanistic studies of azole alkylation reactions mediated by **B** suggest involvement of a Ni(II)/Ni(III) redox couple,[20] we decided to apply our phenanthridine-containing ligand architecture in the preparation of π-extended Ni(II) analogues (**C**) to probe the impact of π-extension on the stability of higher oxidation states[21] and potentially with it, catalytic activity. We report here that complexes of the type **C** are competent in the catalytic C−H bond alkylation of azoles with unactivated alkyl halides containing β-hydrogens, with activity and good substrate scope comparable to **A** and **B** without the requirement of a Cu cocatalyst.

RESULTS AND DISCUSSION

Synthesis and Characterization of Proligands and Their Coordination Complexes. To access the proligands used in this work, aminophenanthridines/quinolines suitable for elaboration into the target scaffolds were prepared. First, (4-nitro)phenanthridines were assembled via tandem cross-coupling/condensation reactions[15,16] to produce **1a−c** (Scheme 1). These were then reduced to the corresponding (4-amino)phenanthridines **2a−c** and coupled with (*N*,*N*-dimethyl)(2-bromo-4-methyl)aniline using Pd-catalyzed C−N bond formation to give proligands **3a−c** as yellow solids, which could be purified using column chromatography. For each of the amine proligands, the hydrogen in the 6-position of the phenanthridine framework resonates significantly downfield of the remaining aromatic resonances in the ^{1}H NMR spectrum, indicating formation of the tricyclic phenanthridine.[22] The appearance of a broad singlet assigned to an N−*H* signal similarly confirmed formation of the diarylamine unit. For comparison, the (6-methyl)quinolinyl analogue **5** was also prepared via Pd-catalyzed C−N coupling.

The solid-state structures of the phenanthridine-containing proligands **3a−c** were determined using single crystal X-ray diffraction (Figure 2). Consistent with the general importance of "imine-bridged biphenyl" resonance contributors to the ground-state structure of phenanthridines,[23] the C−N distance between the phenanthridinyl nitrogen and the adjacent carbon in the 6-position is quite short in all three proligands [**3a**:

https://dx.doi.org/10.1021/acs.organomet.0c00161
Organometallics XXXX, XXX, XXX−XXX

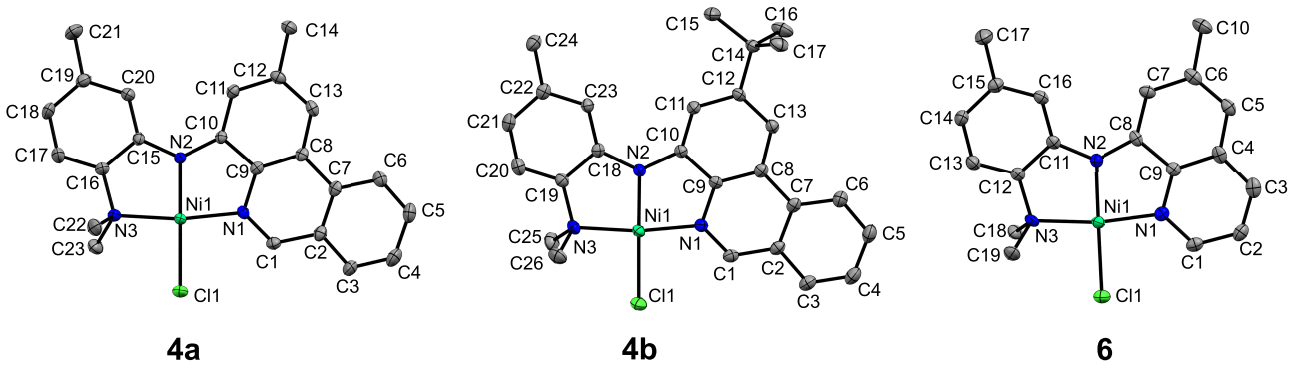

Figure 3. Solid-state structure of **4a**, **4b**, and **6** shown with thermal ellipsoids at 50% probability levels. Hydrogens are omitted for clarity. Selected bond distances (Å) and angles (deg) for **4a**: Ni(1)−Cl(1) 2.1919(8), Ni(1)−N(1) 1.895(2), Ni(1)−N(2) 1.848(2), Ni(1)−N(3) 1.951(2), C(1)−N(1) 1.304(4); N(1)−Ni(1)−N(3) 170.83(10), Cl(1)−Ni(1)−N(2) 179.08(8), N(1)−Ni(1)−N(2) 84.95(10), N(3)−Ni(1)−N(2) 86.35(10), N(1)−Ni(1)−Cl(1) 94.03(7), N(3)−Ni(1)−Cl(1) 93.62(7). **4b**: Ni(1)−Cl(1) 2.1950(5), Ni(1)−N(1) 1.8937(14), Ni(1)−N(2) 1.8511(14), Ni(1)−N(3) 1.9512(15), C(1)−N(1) 1.316(2); N(1)−Ni(1)−N(3) 171.60(6), Cl(1)−Ni(1)−N(2) 176.71(5), N(1)−Ni(1)−N(2) 85.12(6), N(3)−Ni(1)−N(2) 86.49(6), N(1)−Ni(1)−Cl(1) 94.50(5), N(3)−Ni(1)−Cl(1) 93.90(5). **6**: Ni(1)−Cl(1) 2.2094(9), Ni(1)−N(1) 1.896(2), Ni(1)−N(2) 1.859(2), Ni(1)−N(3) 1.949(2), C(1)−N(1) 1.326(4); N(1)−Ni(1)−N(3) 170.93(10), Cl(1)−Ni(1)−N(2) 176.84(8), N(1)−Ni(1)−N(2) 84.69(10), N(3)−Ni(1)−N(2) 86.25(10), N(1)−Ni(1)−Cl(1) 94.59(8), N(3)−Ni(1)−Cl(1) 94.42(7).

C(1)−N(1) 1.3034(11); **3b**: C(1)−N(1) 1.302(3); **3c**: C(1)−N(1) 1.291(4)] pointing to localization of imine C=N character at this site.[18] The localization of imine C=N π character at this site has been shown to temper the impacts of π-extension, for example, in emissive complexes of phenanthridinyl-based ligands.[22,24]

With the proligands in hand, Ni(II) coordination complexes **4a−c** and the quinoline congener **6** were synthesized through metalation with $NiCl_2{\cdot}6H_2O$ in the presence of base (sodium *tert*-butoxide) in dichloromethane at elevated temperatures, and isolated in good yields (83−93%) as dark red solids. The disappearance of the signal assigned to the N−*H* resonance in the ^{1}H NMR spectrum and shifts to the remaining signals, including the diagnostic signals for the hydrogen nucleus in the 6-position of the phenanthridinyl/quinolinyl arms, confirmed installation of the ligand frameworks on the Ni(II) ion. The geometry and structures of the (*N*^*N*^*N*)NiCl complexes were determined using single-crystal X-ray diffraction (Figure 3). In keeping with analogous complexes such as **B**,[10] the nickel ions in **4a**,**b** and **6** sit within the meridional pocket formed by the *N*^*N*^*N* diarylamido ligand. All complexes are essentially flat (angles between planes formed by six carbon rings (e.g., C8−C13 and C15−C20 for **4a**) flanking the amido nitrogens: **4a** 9.43°, **4b** 3.49°, **6** 10.42°), but with distorted square-planar geometry resulting from tied-back bond angles formed by the two neutral donor arms [**4a**: N(1)−Ni(1)−N(3) 170.83(10); **4b**: N(1)−Ni(1)−N(3) 171.60(6); **6**: N(1)−Ni(1)−N(3) 170.93(10)°]. The Ni−N_{amido} distances (**4a**: 1.848(2); **4b**: 1.8511(14); **6**: 1.859(2) Å] are within range of those reported for **A**[25] and **B**,[10] and shorter than between nickel and the neutral donor arms [**4a**: Ni(1)−N(1) 1.895(2), Ni(1)−N(3) 1.951(2); **4b**: Ni(1)−N(1) 1.8937(14), Ni(1)−N(3) 1.9512(15); **6**: Ni(1)−N(1) 1.896(2), Ni(1)−N(3) 1.949(2) Å]. For these latter Ni−N distances, the Ni−NMe_2 distance is consistently longer than the Ni−$N_{heterocycle}$ distance. All three complexes show similar Ni−Cl distances (~2.2 Å), implying very similar *trans* influence to the amido nitrogens of the ligand frameworks.

Catalytic Activity. We then screened the prepared coordination complexes for reactivity in the direct C−H activation of azoles using unactivated alkyl halides (Table 1).

Table 1. Catalyst Comparison for [Ni]-Catalyzed Alkylation of Benzannulated Azoles[a]

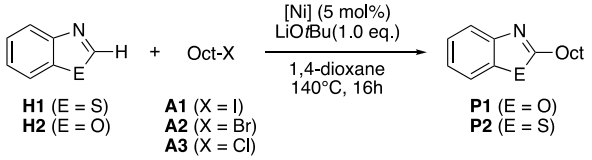

entry	catalyst	heterocycle	alkyl halide	yield[b]
1	**4a**	H1	A1	49
2	**4b**	H1	A1	49
3	**4c**	H1	A1	42
4	**6**	H1	A1	61
5	**4a**	H2	A1	46
6	**4b**	H2	A1	39
7	**4c**	H2	A1	73
8[c]	**4c**	H2	A1	63
9[d]	**4c**	H2	A1	55
10[e]	**4c**	H2	A1	65
11[f]	**4c**	H2	A1	0
12	**6**	H2	A1	39
13	**4c**	H2	A2	35
14[g]	**4c**	H2	A2	57
15[g]	**4c**	H2	A3	87

[a]Conditions unless otherwise specified: heterocycle (1.006 mmol), alkyl halide (1.509 mmol), LiO*t*Bu (1.06 mmol), solvent (2.0 mL); oil bath set to 140 °C, 16 h. [b]GC yield; average of two runs. [c]In the presence of 100 equiv of elemental Hg. [d]In the presence of 500 equiv of elemental Hg. [e]Reaction mixture filtered after 1 h. [f]In the presence of added TEMPO. [g]With 0.2 equiv of NaI.

Comparing all four precatalysts, the 6-methyl substituted quinolinyl congener **6**, a direct analogue of **B**,[10] was found to give the highest yield (61%, run 4) in the direct alkylation of benzothiazole (**H1**) with iodooctane (**A1**) using 5 mol % catalyst loading, 1 equiv of LiO*t*Bu, 1,4-dioxane solvent and 16 h reaction time at 140 °C. As noted, complex **B** has been previously shown to be highly competent in the coupling of alkyl halides with sulfur-containing benzothiazoles.[10] Phenanthridinyl-based analogues **4a−c** were competitive, but gave slightly lower yields (42−49%; runs 1−3) under these

https://dx.doi.org/10.1021/acs.organomet.0c00161
Organometallics XXXX, XXX, XXX−XXX

Table 2. Scope for 4c Catalyzed Alkylations of Benzoxazole with Alkylbromides[a]

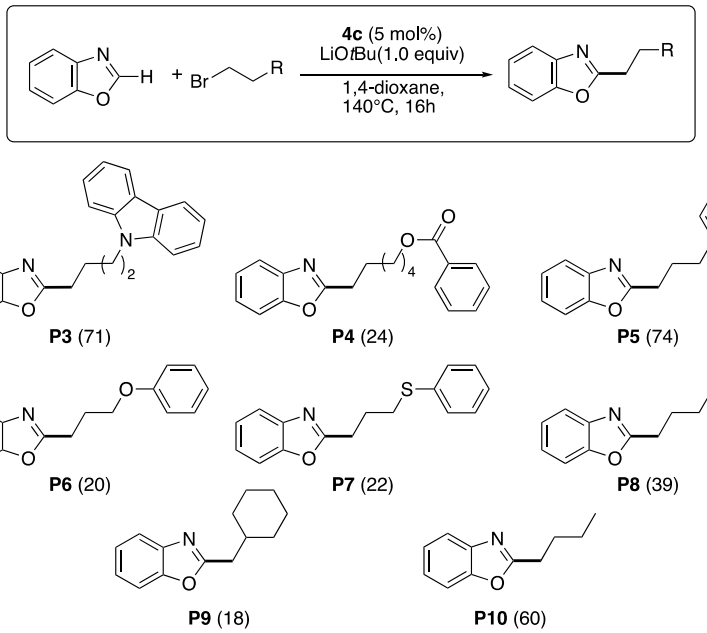

[a]Conditions: heterocycle (1.006 mmol), 1-bromoalkane (1.509 mmol), LiO*t*Bu (1.060 mmol), solvent (2.0 mL); 140 °C, 16 h; GC yield in parentheses.

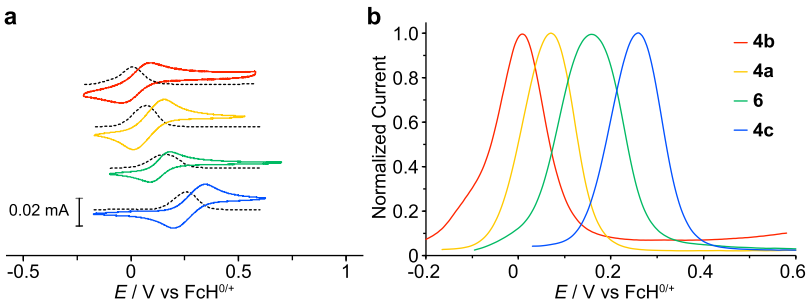

Figure 4. (a) Cyclic voltammograms (solid line) and corresponding differential pulse voltammograms (dashed line) of **4a−c** and **6** in CH_2Cl_2 with 0.10 M $[nBu_4N][PF_6]$ as the supporting electrolyte, glassy carbon working electrode. CV scan rates were 100 mV/s. Potentials are referenced vs the $FcH^{0/+}$ redox couple (FcH = ferrocene). (b) Normalized DPVs of **4a−c** and **6**.

conditions. In the coupling of alkyl halides with the oxygen-containing starting material benzoxazole (**H2**), **4c** began to significantly outperform all other precatalysts. Yields of the coupled product were found to reach as high as 87% using octyl chloride (**A3**) in the presence of NaI.

Having observed promising reactivity with benzannulated coordination complex **4c**, we next explored a brief substrate scope for **4c** as precatalyst (Table 2). The reaction conditions were found to be amenable to the coupling of benzoxazole with a variety of alkyl halides bearing carbazole (**P3**), ester (**P4**), aryl (**P5**), arylether (**P6**), thioether (**P7**), alkenyl (**P8**), and aliphatic (**P9**, **P10**) substituents. The catalysis mediated by **4a−c** and **6** likely proceeds analogously to what has been observed by Punji and co-workers using their related quinolinyl-supported precatalyst **B**.[10,20] In support of this, participation of heterogeneous particulate nickel generated via catalyst decomposition appears to be minimal, as catalysis in the presence of added Hg (Table 1, runs 8−9) and following filtration (run 10) proceeded unimpeded. On the other hand, addition of the radical scavenger TEMPO (2,2,6,6-tetramethylpiperidine 1-oxyl) completely shut down reactivity (run 11). This is consistent with the homogeneous radical rebound pathway proposed by Punji and co-workers, which involves on-cycle high-valent Ni(III) and Ni(IV) intermediates.[20] Accordingly, we collected electrochemical data for the precatalysts screened in this work in an attempt to correlate catalytic behavior with redox potentials.

Cyclic voltammograms (CVs) and differential pulse voltammograms (DPVs) of precatalysts **4a−c** and **6** were taken in dichloromethane solution with 0.1 M $[nBu_4N][PF_6]$ as the supporting electrolyte (Figure 4). A quasi-reversible anodic wave between 0 and +0.3 V (vs $FcH^{0/+}$; FcH = ferrocene) is observed for each compound, consistent with an overall $1e^-$ oxidation. All compounds exhibit broad, irreversible reductions that overlap with the edge of the solvent window, making comparisons of these cathodic features within the series challenging. Accordingly, we focus here on the anodic electrochemical events. The oxidation potentials and peak parameters for the complexes are tabulated in Table 3. The electron releasing *t*Bu group of **4b** shifts the oxidation potential to more accessible potentials compared with methyl analogues **4a** and **6**. In comparison, an anodically shifted oxidation is observed for **4c**, consistent with the presence of an electron withdrawing substituent on the ligand. The alkylation pathway

https://dx.doi.org/10.1021/acs.organomet.0c00161
Organometallics XXXX, XXX, XXX−XXX

Table 3. Electrochemical Parameters for Ni Complexes

compound	$E_{1/2}$ (V)	Δ_{ptp}[a] (mV)	i_{red}/i_{ox}
4b	0.01	133	1.17
4a	0.07	143	1.04
6	0.16	91	0.87
4c	0.26	147	0.92

[a]Δ_{ptp} = distance measured from "peak-to-peak", showing the separation in mV between the peak maximum of the oxidation and corresponding reduction.

catalyzed by **B** proposed by Punji and co-workers[20] invokes a one-electron Ni(II/III) pathway that occurs by oxidative addition of alkyl iodide via iodine atom transfer (IAT).[26] The lack of reactivity in the presence of the radical trap TEMPO (Table 1, run 11) supports a similar mechanism here. Oxidative addition by (inner-sphere) electron-transfer mechanisms are typically associated with metal centers with coordinative unsaturation to bind a substrate, and sufficiently cathodic electrochemical potentials to reduce the organic electrophile.[27] The observation of higher yields for the most electrophilic congener **4c** with a pronounced anodic shift to its oxidation event suggests that the elevated π-acidicity of the CF_3-substituted phenanthridine ligand framework[18] may be key in this context.

CONCLUSION

In conclusion, we have demonstrated that the introduction of benzannulated phenanthridine ligands supporting Ni(II) coordination complexes maintain the high activity observed in the C−H alkylation of azoles observed with quinoline congeners,[10] for both benzoxazole and benzothiazole. The synthetic route to the *N^N(H)^N* proligand frameworks **3a−c** allows for facile incorporation of different substituents, whose electron-releasing/electron-withdrawing properties can be quantified in terms of the redox properties of their Ni complexes in solution. Comprehensive mechanistic studies, including investigating correlation of catalytic activity to the π-acidity of the benzannulated phenanthridine ligand frameworks,[18] and expansion of the scope of C−C bond forming reactions to other substrate classes is presently underway.

EXPERIMENTAL SECTION

Unless otherwise specified, air sensitive manipulations were carried either in an N_2-filled glovebox or using standard Schlenk techniques under Ar. (*N,N*-Dimethyl)-*para*-toluidine (Sigma-Aldrich), 2-formylphenyl boronic acid (AK Scientific), *N*-iodosuccinimide (AK Scientific), *N*-bromosuccinimide (Alfa Aesar), $Pd(PPh_3)_4$ (Sigma-Aldrich), $Pd_2(dba)_3$ (Sigma-Aldrich), 2-nitro-4-(trifluoromethyl)-aniline (Sigma-Aldrich), (1,1′-diphenylphosphino)ferrocene (dppf, Sigma-Aldrich), (±)-2,2′-bis(diphenylphosphino)-1,1′-binapthalene (*rac*-BINAP, Sigma-Aldrich), Na_2CO_3 (Alfa Aesar), trifluoroacetic acid (Sigma-Aldrich), sodium *tert*-pentoxide (NaO*t*Am, Sigma-Aldrich), sodium *tert*-butoxide (NaO*t*Bu, Sigma-Aldrich), zinc (Alfa Aesar), hydrazine hydrate (Sigma-Aldrich), formic acid (Alfa Aesar), $NiCl_2{\cdot}6H_2O$ (Alfa Aesar), and all reagents used in precursor synthesis and catalytic trials were purchased and used without any further purification. (2-Bromo-4,*N*,*N*-trimethyl)aniline,[28] (8-amino-4-methyl)quinoline,[29] (4-amino-2-methyl)phenanthridine (**2a**),[15] (4-amino-2-*tert*-butyl)phenanthridine (**2b**),[18] and 2-iodo-6-nitro-4-trifluoromethylaniline[30] were synthesized according to published procedures. Organic solvents were dried and distilled using appropriate drying agents, while distilled water was degassed prior to use. Multinuclear 1D and 2D NMR spectra were recorded on Bruker Avance 300 MHz or Bruker Avance III 500 MHz spectrometers. ^1H and $^{13}C\{^1H\}$ NMR spectra were referenced to residual solvent peaks. Elemental analyses were performed by Microanalytical Service Ltd., Delta, BC, Canada, and at the University of Manitoba using a PerkinElmer 2400 Series II CHNS/O Elemental Analyzer. High-resolution mass spectra were recorded using a Bruker microOTOF-QIII.

Synthesis of 4-Nitro-2-trifluoromethylphenanthridine (1c). A 500 mL Teflon-stoppered flask was charged with $Pd(PPh_3)_4$ (1.04 g, 0.90 mmol), and 50 mL of 1,2-dimethoxyethane (DME). After stirring briefly to mix, 2-iodo-6-nitro-4-trifluoromethylaniline (10.0 g, 30.1 mmol), 2-formylphenylboronic acid (4.97 g, 33.1 mmol), and an additional 70 mL of DME were added, followed by Na_2CO_3 (9.6 g, 90.4 mmol) dissolved in 100 mL of degassed water. The flask was then sealed and the mixture stirred vigorously for 6 h in an oil bath set to 130 °C. The flask was then allowed to cool, charged with 130 mL of 2 M HCl, and refluxed for additional 2 h. The reaction mixture was cooled, neutralized with NaOH, and pumped to dryness. The residue was then taken up in dichloromethane (100 mL) and washed with brine (3 × 100 mL). The organic layer was separated, dried over Na_2SO_4 and volatiles removed. Column chromatography on neutral alumina gave a pale yellow solid (R_f = 0.41; 1:5 EtOAc/hexanes). Isolated yield = 7.86 g (89%). ^1H NMR ($CDCl_3$, 300 MHz, 22 °C) δ 9.48 (s, 1H; $C_{Ar}H$), 9.01 (s, 1H; $C_{Ar}H$), 8.67 (d, 1H, J_{HH} = 8.0 Hz; $C_{Ar}H$), 8.18 (overlapped m, 2H; $C_{Ar}H$), 8.05 (ddd, 1H, J_{HH} = 8.4, 7.2, 1.4 Hz; $C_{Ar}H$), 7.92 ppm (m, 1H; $C_{Ar}H$). $^{13}C\{^1H\}$ NMR ($CDCl_3$, 125 MHz, 22 °C):δ 158.0 (C_{Ar}), 149.8 (C_{Ar}), 137.5 (C_{Ar}), 133.1 (C_{Ar}), 131.2 (q, C_{Ar}), 130.0 (C_{Ar}), 129.8 (C_{Ar}), 128.4 (C_{Ar}), 126.9 (C_{Ar}), 126.0 (C_{Ar}), 124.3 (C_{Ar}), 123.2 (q, CF_3), 122.3 (C_{Ar}), 118.7 ppm (q, C_{Ar}). $^{19}F\{^1H\}$ NMR ($CDCl_3$, 282 MHz, 22 °C) δ −62.03 ppm.

4-Amino-2-trifluoromethylphenanthridine (2c). To a stirred solution of **1c** (6.02 g, 20.5 mmol) in methanol (100 mL), Zn dust (2.68 g, 41.1 mmol), and hydrazinium monoformate solution (54 mL; prepared by slowly neutralizing equal molar amounts of hydrazine hydrate (50 mL) with 85% formic acid (4 mL) in an ice−water bath) were added and stirred vigorously at 60 °C. The resulting green suspension was cooled and filtered over Celite. The filtrate was pumped dry, the residue dissolved in dichloromethane (100 mL), and washed with brine (3 × 60 mL). The organic layer was separated, dried over Na_2SO_4, and dried to leave a brown solid. Column chromatography on neutral alumina gave a pale-yellow solid (R_f = 0.43; 1:5 EtOAc/hexane). Isolated yield = 3.74 g (86%). ^1H NMR ($CDCl_3$, 300 MHz, 22 °C) δ 9.15 (s, 1H; $C_{Ar}H$), 8.50 (d, 1H, J_{HH} = 8.3; $C_{Ar}H$), 8.07 (s, 1H; $C_{Ar}H$), 8.01 (dd, 1H, J_{HH} = 8.0, 1.3 Hz; $C_{Ar}H$), 7.83 (app t, 1H, J_{HH} = 8.4, 7.0 Hz; $C_{Ar}H$), 7.70 (app t, 1H, J_{HH} = 8.1, 7.0; $C_{Ar}H$), 7.13 (d, 1H, J_{HH} = 1.8 Hz; $C_{Ar}H$), 5.22 ppm (br s, 2H; N*H*). $^{13}C\{^1H\}$ NMR ($CDCl_3$, 75 MHz, 22 °C) δ 152.2 (C_{Ar}), 145.6 (C_{Ar}), 134.5 (C_{Ar}), 132.7 (C_{Ar}), 131.3 (q, C_{Ar}), 128.9 (C_{Ar}), 128.1 (C_{Ar}), 126.9 (C_{Ar}), 124.3 (C_{Ar}), 122.5 (C_{Ar}), 107.9 (q, CF_3), 106.7 ppm (q, C_{Ar}). $^{19}F\{^1H\}$ NMR ($CDCl_3$, 282 MHz, 22 °C) δ −62.28 ppm.

Synthesis of ^{Me}QuinNN(H)NMe$_2$ (5).

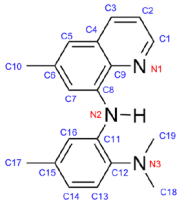

A 350 mL Teflon-stoppered flask was charged with $Pd_2(dba)_3$ (1.91 g, 2.09 mmol), dppf (2.69 g, 4.69 mmol), and toluene (30 mL). After stirring briefly, (8-amino-4-methyl)quinoline[29] (4.15 g, 26.1 mmol), (2-bromo-4,*N*,*N*-trimethyl)aniline[28] (6.70 g, 31.3 mmol) were combined with an additional 90 mL of toluene, followed by NaO*t*Am (4.30 g, 39.1 mmol). The mixture was then stirred vigorously for 72 h in an oil bath set to 130 °C. After cooling the flask and removing the volatiles, the residue was taken up in dichloromethane (120 mL), and the resulting suspension filtered over Celite and dried. Column chromatography gave a yellow oil which solidified on standing

https://dx.doi.org/10.1021/acs.organomet.0c00161
Organometallics XXXX, XXX, XXX−XXX

(neutral alumina; 1:10 EtOAc/hexane; R_f = 0.5). Isolated yield = 8.23 g (74%). ^{1}H NMR ($CDCl_3$, 500 MHz, 22 °C) δ 8.76 (dd, 1H; J_{HH} = 4.2, 1.7 Hz, C_1H), 8.65 (brs, 1H; NH), 8.01 (dd, 1H, J_{HH} = 8.3, 1.7 Hz; C_3H), 7.50 (d, 1H, J_{HH} = 1.9 Hz; $C_{16}H$), 7.46 (d, 1H, J_{HH} = 1.7 Hz; C_7H), 7.38 (dd, 1H, J_{HH} = 8.2, 4.2 Hz; C_2H), 7.06 (d, 1H, J_{HH} = 8.0 Hz; $C_{13}H$), 7.00 (s, 1H, C_5H), 6.81 (m, 1H, J_{HH} = 8.0, 2.0 Hz; $C_{14}H$), 2.72 (s, 6H; N($C_{(18,19)}H_3$)$_2$), 2.51 (s, 3H; $C_{10}H_3$), 2.38 (s, 3H, $C_{17}H_3$). ^{13}C{^{1}H} NMR ($CDCl_3$, 125 MHz, 22 °C) δ 146.7(C_1), 142.7 (C_{12}), 139.7 (C_8), 138.1 (C_9), 137.3 (C_6), 136.0 (C_{11}), 136.0 (C_3), 132.7 (C_{15}), 129.1 (C_4), 122.1 (C_{14}), 121.6 (C_2), 119.2 (C_{13}), 118.5 (C_{16}), 115.5 (C_5), 109.6 (C_7), 44.1 (N($C_{18,19}$)$_2$), 22.5 (C_{10}), 21.4 ppm (C_{17}).

Synthesis of ^{Me}PhenNN(H)NMe$_2$ (3a).

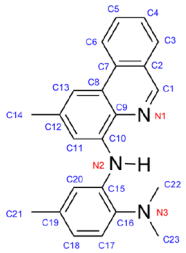

An identical procedure to the synthesis of **5** was employed, using $Pd_2(dba)_3$ (0.51 g, 0.55 mmol), dppf (0.67 g, 1.21 mmol), **2a** (2.30 g, 11.0 mmol), (2-bromo-4,*N*,*N*-trimethyl)aniline[28] (2.83 g, 13.3 mmol) and NaO*t*Am (1.82 g, 16.6 mmol). Column chromatography on neutral alumina gave a yellow solid (1:10 EtOAc/hexane; R_f = 0.5). Isolated yield = 1.34 g (97%). ^{1}H NMR ($CDCl_3$, 500 MHz, 22 °C) δ 9.18 (s, 1H; C_1H), 8.72 (br s, 1H; NH), 8.61 (d, 1H, J_{HH} = 8.2 Hz; C_6H), 8.06 (d, 1H, J_{HH} = 7.7 Hz; C_3H), 7.84 (dd, 1H, J_{HH} = 8.4, 7.0 Hz; C_5H), 7.78 (s, 1H; $C_{20}H$), 7.71 (dd, 1H, J_{HH} = 8.0, 7.0 Hz; C_4H), 7.55 (s, 1H; $C_{13}H$), 7.51(s, 1H; $C_{11}H$), 7.07 (d, 1H, J_{HH} = 8.0 Hz; $C_{17}H$), 6.82 (dd, 1H, J_{HH} = 8.0, 1.9 Hz; $C_{18}H$), 2.74 (s, 6H; N($C_{22,23}H_3$)$_2$), 2.60 (s, 3H; $C_{14}H_3$), 2.38 ppm (s, 3H; $C_{21}H_3$). ^{13}C{^{1}H} NMR ($CDCl_3$, 75 MHz, 22 °C) δ 149.5 (C_1), 142.7 (C_{16}), 140.7 (C_{10}), 137.7 (C_{12}), 136.1 (C_{15}), 132.8 (C_9), 132.7 (C_{19}), 132.6 (C_2), 130.5 (C_5), 128.6 (C_3), 127.3 (C_4), 127.1 (C_8), 124.7 (C_7), 122.4 (C_6), 122.0 (C_{18}), 119.1 (C_{17}), 118.7 (C_{11}), 111.0 (C_{20}), 110.5 (C_{13}), 44.1 (N($C_{22,23}$)$_2$), 22.8 (C_{14}), 21.3 ppm (C_{21}).

Synthesis of ^{tBu}PhenNN(H)NMe$_2$ (3b).

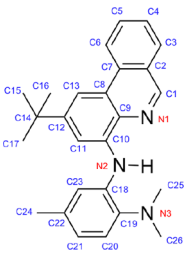

An identical procedure to the synthesis of **5** was employed, using $Pd_2(dba)_3$ (0.55 g, 0.60 mmol), dppf (0.73 g, 1.32 mmol), **2b** (3.0 g, 11.9 mmol), (2-bromo-4,*N*,*N*-trimethyl)aniline[28] (2.87 g, 13.4 mmol), and NaO*t*Am (1.98 g, 17.9 mmol). Column chromatography on neutral alumina gave a yellow solid (1:10 EtOAc/hexane; R_f = 0.5). Isolated yield = 4.18 g (91%) ^{1}H NMR ($CDCl_3$, 300 MHz, 22 °C) δ 9.18 (s, 1H; C_1H), 8.73 (brs, 1H; NH), 8.65 (d, 1H, J_{HH} = 8.4 Hz; C_6H), 8.11−7.97 (m, 2H; C_3H, $C_{23}H$), 7.96−7.80 (m, 2H; C_5H, $C_{13}H$), 7.69 (m, 1H; C_4H), 7.54 (s, 1H; $C_{11}H$), 7.08 (dd, 1H, J_{HH} = 8.0, 2.5 Hz; $C_{20}H$), 6.80 (dd, 1H, J_{HH} = 8.1, 2.2 Hz; $C_{21}H$), 2.78 (s, 6H; N($C_{25,26}H_3$)$_2$), 2.37 (s, 3H; $C_{24}H_3$), 1.52 ppm (s, 9H; ($C_{15,16,17}H_3$)$_3$). ^{13}C{^{1}H} NMR ($CDCl_3$, 75 MHz, 22 °C) δ 150.6 (C_{12}), 150.0 (C_1), 142.3 (C_{19}), 140.1 (C_{10}), 136.6 (C_{18}), 133.2 (C_9), 133.1 (C_2), 132.9 (C_{22}), 130.6 (C_5), 128.8 (C_3), 127.2 (C_4), 127.0 (C_8), 124.3 (C_7), 122.4 (C_6), 121.5 (C_{21}), 119.3 (C_{20}), 117.4 (C_{11}), 108.9 (C_{23}), 107.4 (C_{13}), 44.2 (N($C_{25,26}$)$_2$), 35.7 (C_{14}), 31.7 ($C_{15,16,17}$), 21.5 ppm (C_{24}).

Synthesis of ^{CF3}PhenNN(H)NMe$_2$ (3c).

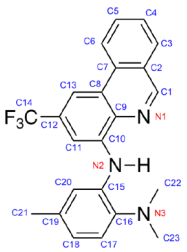

An identical procedure to the synthesis of **5** was employed, using $Pd_2(dba)_3$ (0.20 g, 0.22 mmol), dppf (0.27 g, 0.49 mmol), **2c** (1.16 g, 4.42 mmol), (2-bromo-4,*N*,*N*-trimethyl)aniline[28] (1.14 g, 5.30 mmol) and NaO*t*Am (0.73 g, 6.63 mmol). Column chromatography on neutral alumina gave a yellow solid (1:10 EtOAc/hexane; R_f = 0.5). Isolated yield = 1.50 g (85%) ^{1}H NMR ($CDCl_3$, 300 MHz, 22 °C) δ 9.30 (s, 1H; C_1H), 8.89 (brs, 1H; NH), 8.63 (d, 1H, J_{HH} = 8.3 Hz; C_6H), 8.18 (s, 1H; $C_{13}H$), 8.11 (d, 1H, J_{HH} = 8.0 Hz; C_3H), 7.92 (t, 1H, J_{HH} = 8.3, 6.9 Hz; C_5H), 7.83−7.73 (m, 2H; C_4H, $C_{11}H$), 7.46 (s, 1H, $C_{20}H$) 7.07 (d, 1H, J_{HH} = 8.0, Hz; $C_{17}H$), 6.87 (d, 1H, J_{HH} = 8.2; $C_{18}H$), 2.72 (s, 6H; N($C_{22,23}H_3$)$_2$), 2.37 ppm (s, 3H; $C_{21}H_3$). ^{13}C{^{1}H} NMR ($CDCl_3$, 125 MHz, 22 °C) δ 152.3 (C_1), 143.2 (C_{10}), 141.9 (C_{16}), 135.2 (C_{15}), 135.1 (C_9), 133.1 (C_2), 133.0 (C_{19}), 131.5 (C_5), 129.6 (C_{14}, quartet), 129.0 (C_3), 128.2 (C_4), 127.1 (C_{12}), 125.8 (C_8), 123.7 (C_7), 123.3 (C_{18}), 122.6 (C_6), 119.5 (C_{17}), 119.4 (C_{20}), 108.0 (C_{13}), 104.2 (C_{11}), 44.14 (N($C_{22,23}$)$_2$), 21.4 ppm (C_{21}). ^{19}F{^{1}H} NMR ($CDCl_3$, 282 MHz, 22 °C) δ −62.37 ppm (s, 3F; CF_3).

Synthesis of ^{Me}QuinNNNMe$_2$-Ni (6).

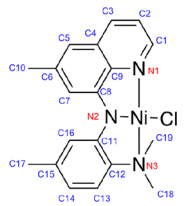

To a stirred solution of compound **5** (1.01 g, 3.43 mmol) in 30 mL of dichloromethane, $NiCl_2{\cdot}6H_2O$ (0.86g, 3.60 mmol), and NaO*t*Bu (0.35 g, 3.60 mmol) were added, and the mixture stirred vigorously at 65 °C for 18 h. The resulting red suspension was allowed to cool, and the volatiles removed in vacuo. The residue was then washed with diethyl ether (3 × 15 mL) to isolate red solid. The compound is further purified by redissolving in DCM and passed through Celite. Isolated yield = 1.17 g (89%). ^{1}H NMR ($CDCl_3$, 500 MHz, 22 °C) δ 8.46 (d, 1H, J_{HH} = 5.0 Hz; C_1H), 7.98 (dd, 1H, J_{HH} = 8.2, 1.5 Hz; C_3H), 7.34 (s, 1H; $C_{16}H$), 7.24 (s, 1H; $C_{7/5}H$), 7.17 (dd, 1H, J_{HH} = 8.2, 5.3 Hz; C_2H), 6.96 (d, 1H, J_{HH} = 8.1; $C_{13}H$), 6.67 (s, 1H; $C_{5/7}H$), 6.47−6.40 (m, 1H; $C_{14}H$), 3.02 (s, 6H; N($C_{19,18}H_3$)$_2$), 2.48 (s, 3H; $C_{10}H_3$), 2.36 ppm (s, 3H; $C_{17}H_3$). ^{13}C{^{1}H} NMR ($CDCl_3$, 125 MHz, 22 °C) δ 149.5 (C_1), 147.9 (C_8), 147.2 (C_{11}), 146.1 (C_9), 145.2 (C_{12}), 139.6 (C_6), 138.5 (C_{15}), 137.7 (C_3), 129.5 (C_4), 120.9 (C_2), 119.9 (C_{13}), 117.9 (C_{14}), 115.5 (C_{16}), 112.5 ($C_{5/7}$), 112.3 ($C_{5/7}$), 51.9 (N($C_{18,19}$)$_2$), 22.6 (C_{10}), 21.7 ppm (C_{17}). Anal. Calcd for $C_{19}H_{20}ClN_3Ni$: C, 59.35; H, 5.24. Found: C, 59.07; H, 5.25.

Synthesis of ^{Me}PhenNNNMe$_2$-Ni (4a).

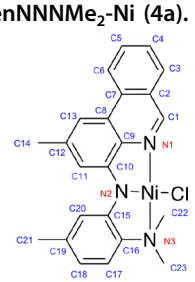

An identical procedure to the synthesis of **6** was employed, using **3a** (1.14 g, 3.33 mmol), $NiCl_2{\cdot}6H_2O$ (0.81 g, 3.42 mmol), and NaO*t*Bu (0.34 g, 3.50 mmol) in 15 mL of dichloromethane. Isolated yield =

https://dx.doi.org/10.1021/acs.organomet.0c00161
Organometallics XXXX, XXX, XXX−XXX

1.32 g (91%). ^{1}H NMR ($CDCl_3$, 300 MHz, 22 °C) δ 8.88 (s, 1H; C_1H), 8.39 (d, 1H, J_{HH} = 8.4 Hz; C_6H), 7.88 (d, 1H, J_{HH} = 8.1 Hz; C_3H), 7.83 (t, 1H, J_{HH} = 7.8 Hz; C_5H), 7.61 (t, 1H, J_{HH} = 7.6 Hz; C_4H), 7.37 (s, 1H; $C_{20}H$), 7.31 (s, 1H; $C_{11}H$), 7.28 (s, 1H; $C_{13}H$), 6.96 (d, 1H, J_{HH} = 8.1 Hz; $C_{17}H$), 6.43 (d, 1H, J_{HH} = 7.8 Hz; $C_{18}H$), 3.05 (s, 6H; $N(C_{22,\ 23}H_3)_2$), 2.57 (s, 3H; $C_{14}H_3$), 2.36 ppm (s, 3H; $C_{21}H_3$). $^{13}C\{^1H\}$ NMR ($CDCl_3$, 125 MHz, 22 °C) δ 153.9 (C_1), 148.5 (C_{10}), 147.3 (C_{15}), 145.0 (C_{16}), 140.0 (C_9), 139.6 (C_{12}), 138.3 (C_{19}), 132.7 (C_2), 132.4 (C_5), 129.6 (C_3), 127.5 (C_4), 126.0 (C_8), 125.2 (C_7), 122.2 (C_6), 119.8 (C_{17}), 117.6 (C_{18}), 115.4 (C_{20}), 112.2 (C_{11}), 108.3 (C_{13}), 51.8 ($N(C_{22,\ 23})_2$), 22.8 (C_{14}) and 21.6 (C_{21}). Anal. Calcd for $C_{23}H_{22}ClN_3Ni$: C, 63.57; H, 5.10. Found: C, 63.60; H, 5.21.

Synthesis of ^{tBu}PhenNNNMe$_2$-Ni (4b).

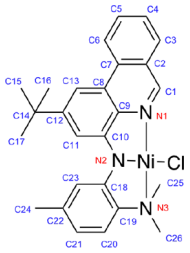

An identical procedure to the synthesis of **6** was employed, using **3b** (1.01 g, 2.60 mmol), $NiCl_2{\cdot}6H_2O$ (0.65 g, 2.74 mmol), and NaO*t*Bu (0.26 g, 2.74 mmol) in 15 mL of dichloromethane. Isolated yield = 1.17 g (93%). ^{1}H NMR ($CDCl_3$, 500 MHz, 22 °C) δ 8.93 (s, 1H; C_1H), 8.51 (d, 1H, J_{HH} = 8.3 Hz; C_6H), 7.94 (d, 1H, J_{HH} = 8.1 Hz; C_3H), 7.88 (t, 1H, J_{HH} = 8.1 Hz; C_5H), 7.64 (m, 2H; $C_{4,\ 11/13}H$), 7.55 (s, 1H; $C_{11/13}H$), 7.40 (s, 1H; $C_{23}H$), 6.98 (d, 1H, J_{HH} = 8.2 Hz; $C_{20}H$), 6.43 (d, 1H, J_{HH} = 8.2 Hz; $C_{21}H$), 3.05 (s, 6H; $N(C_{25,\ 26}H_3)_2$), 2.36 (s, 3H; $C_{24}H_3$) and 1.49 ppm (s, 9H; $(C_{15,\ 16,\ 17}H_3)_3$). $^{13}C\{^1H\}$ NMR ($CDCl_3$, 125 MHz, 22 °C) δ 154.4 (C_1), 152.9 (C_{12}), 148.4 (C_{10}), 147.5 (C_{18}), 145.2 (C_{19}), 140.1 (C_9), 138.5 (C_{22}), 133.4 (C_2), 132.6 (C_5), 129.9 (C_3), 127.7 (C_4), 126.3 (C_8), 125.0 (C_7), 122.3 (C_6), 120.0 (C_{20}), 117.5 (C_{21}), 115.4 (C_{23}), 109.4 ($C_{11/13}$), 104.7 ($C_{11/13}$), 51.9 ($N(C_{25,\ 26})_2$), 35.7 ($C_{15,\ 16,\ 17}$)$_3$, 31.8 (C_{14}), 21.9 ppm (C_{24}). Anal. Calcd for $C_{26}H_{28}ClN_3Ni$: C, 65.51; H, 5.92. Found: C, 65.35; H, 6.03.

Synthesis of ^{CF3}PhenNNNMe$_2$-Ni (4c).

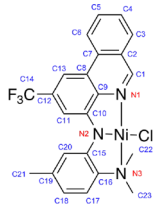

An identical procedure to the synthesis of **6** was employed, using **3c** (1.80 g, 4.56 mmol), $NiCl_2{\cdot}6H_2O$ (1.14 g, 4.77 mmol), and NaO*t*Bu (0.46 g, 4.79 mmol) in 15 mL of dichloromethane. Isolated yield = 1.86 g (83%). ^{1}H NMR ($CDCl_3$, 500 MHz, 22 °C) δ 9.10 (s, 1H; C_1H), 8.48 (d, 1H, J_{HH} = 8.3 Hz; C_6H), 8.10−7.90 (m, 2H; $C_{3,\ 5}H$), 7.84−7.56 (m, 3H; $C_{4,\ 11,\ 13}H$), 7.36 (s, 1H; $C_{20}H$), 7.01 (d, 1H, J_{HH} = 8.2 Hz; $C_{17}H$), 6.52 (d, 1H, J_{HH} = 8.2 Hz; $C_{18}H$), 3.06 (s, 6H; $N(C_{22,23}H_3)_2$), and 2.37 (s, 3H; $C_{21}H_3$). $^{13}C\{^1H\}$ NMR ($CDCl_3$, 125 MHz, 22 °C) δ 156.1 (C_1), 149.0 (C_{10}), 146.5 (C_{15}), 145.3 (C_{16}), 142.6 (C_9), 138.8 (C_{19}), 133.4 (C_5), 132.9 (C_2), 131.1 (C_{14}, quartet), 130.1 (C_3), 128.5 (C_4), 126.1 (C_{12}), 125.5 (C_8), 123.4 (C_7), 122.4 (C_6), 120.1 (C_{17}), 119.0 (C_{18}), 115.8 (C_{20}), 105.9 (C_{13}), 105.1 (C_{11}), 52.0 ($N(C_{22,\ 23})_2$), 21.7 ppm (C_{21}). $^{19}F\{^1H\}$ NMR ($CDCl_3$, 470 MHz, 22 °C) δ −62.27 ppm (s, 3F; CF_3). Anal. Calcd for $C_{23}H_{19}ClF_3N_3Ni$: C, 56.54; H, 3.92. Found: C, 56.33; H, 3.63.

X-ray Crystallography. X-ray crystal structure data was using collected from multifaceted crystals of suitable size and quality selected from a representative sample of crystals of the same habit using an optical microscope. In each case, crystals were mounted on MiTiGen loops with data collection carried out in a cold stream of nitrogen (150 K; Bruker D8 QUEST ECO; Mo Kα radiation). All diffractometer manipulations were carried out using Bruker APEX3 software.[31] Structure solution and refinement was carried out using XS, XT and XL software, embedded within the Bruker SHELXTL suite.[32] For each structure, the absence of additional symmetry was confirmed using ADDSYM incorporated in the PLATON program.[33] CCDC Nos. 1985563−1985568 contain the supplementary crystallographic data for this paper. The data can be obtained free of charge from The Cambridge Crystallographic Data Centre via www.ccdc.cam.ac.uk/structures.

Crystal Structure Data for ***3a*** *(CCDC No. 1985568).* X-ray quality crystals were grown following diffusion of diethyl ether vapor into a saturated $CHCl_3$ solution of the compound at room temperature. Crystal structure parameters: $C_{23}H_{23}N_3$ 341.44 g/mol, monoclinic, space group $P2_1/c$; a = 17.2243(11) Å, b = 14.7273(9) Å, c = 7.1219(5) Å, α = 90°, β = 99.910(3)°, γ = 90°, V = 1779.6(2) Å^3; Z = 4, ρ_{calcd} = 1.274 g cm^{-3}; crystal dimensions 0.266 × 0.200 × 0.150 mm^3; θ_{max} = 39.509°; 114196 reflections, 10645 independent (R_{int} = 0.0597), intrinsic phasing; absorption coeff (μ = 0.076 mm^{-1}), absorption correction semiempirical from equivalents (SADABS); refinement (against F_o^2) with SHELXTL V6.1, 239 parameters, 0 restraints, R_1 = 0.0553 ($I > 2\sigma$) and wR_2 = 0.1722 (all data), GoF = 1.046, residual electron density 0.620/−0.610 e Å^{-3}.

Crystal Structure Data for ***3b*** *(CCDC No. 1985565).* X-ray quality crystals were grown following diffusion of diethyl ether vapor into a saturated $CHCl_3$ solution of the compound at room temperature. Crystal structure parameters: $C_{26}H_{29}N_3$ 383.52 g/mol, trigonal, space group $P3_2$; a = 10.2023(3) Å, b = 10.2023(3) Å, c = 17.7612(6) Å, α = 90°, β = 90°, γ = 120°, V = 1061.03(11) Å^3; Z = 3, ρ_{calcd} = 1.193 g cm^{-3}; crystal dimensions 0.100 × 0.050 × 0.050 mm^3; θ_{max} = 30.499°; 37488 reflections, 6534 independent (R_{int} = 0.0833), intrinsic phasing; absorption coeff (μ = 0.070 mm^{-1}), absorption correction semiempirical from equivalents (SADABS); refinement (against F_o^2) with SHELXTL V6.1, 269 parameters, 1 restraints, R_1 = 0.0533 ($I > 2\sigma$) and wR_2 = 0.1243 (all data), GoF = 1.032, residual electron density 0.294/−0.245 e Å^{-3}.

Crystal Structure Data for ***3c*** *(CCDC No. 1985563).* X-ray quality crystals were grown following diffusion of diethyl ether vapor into a $CHCl_3$ solution of the compound at room temperature. Crystal structure parameters: $C_{23}H_{20}F_3N_3$ 395.42 g/mol, triclinic, space group $P\bar{1}$; a = 7.8443(4) Å, b = 9.5831(4) Å, c = 13.4612(6) Å, α = 89.4932(18)°, β = 78.5285(18)°, γ = 87.8849(19)°, V = 991.02(8) Å^3; Z = 2, ρ_{calcd} = 1.325 g cm^{-3}; crystal dimensions 0.280 × 0.150 × 0.040 mm^3; θ_{max} = 27.721°; 23306 reflections, 4645 independent (R_{int} = 0.0560), intrinsic phasing; absorption coeff (μ = 0.099 mm^{-1}), absorption correction semiempirical from equivalents (SADABS); refinement (against F_o^2) with SHELXTL V6.1, 265 parameters, 0 restraints, R_1 = 0.0793 ($I > 2\sigma$) and wR_2 = 0.2179 (all data), GoF = 1.050, residual electron density 1.031/−0.771 e Å^{-3}.

Crystal Structure Data for ***4a*** *(CCDC No. 1985564).* X-ray quality crystals were grown following diffusion of diethyl ether vapor into a $CHCl_3$ solution of the compound at room temperature. Crystal structure parameters: $C_{23}H_{22}Cl_1N_3Ni_1$ 434.59 g/mol, triclinic, space group $P\bar{1}$; a = 6.9170(4) Å, b = 11.9707(8) Å, c = 12.3017(11) Å, α = 72.668(3)°, β = 82.739(3)°, γ = 89.465(3)°, V = 964.12(11) Å^3; Z = 2, ρ_{calcd} = 1.497 g cm^{-3}; crystal dimensions 0.200 × 0.100 × 0.030 mm^3; θ_{max} = 27.979°; 39487 reflections, 4613 independent (R_{int} = 0.0453), intrinsic phasing; absorption coeff (μ = 1.159 mm^{-1}), absorption correction semiempirical from equivalents (SADABS); refinement (against F_o^2) with SHELXTL V6.1, 257 parameters, 0 restraints, R_1 = 0.0424 ($I > 2\sigma$) and wR_2 = 0.1011 (all data), GoF = 1.137, residual electron density 0.806/−0.637 e Å^{-3}.

Crystal Structure Data for ***4b*** *(CCDC No. 1985566).* X-ray quality crystals were grown following diffusion of diethyl ether vapor into a $CHCl_3$ solution of the compound at room temperature. Crystal structure parameters: $C_{26}H_{28}Cl_1N_3Ni_1$ 476.67 g/mol, monoclinic, space group $P2_1/c$; a = 14.9402(10) Å, b = 16.7884(11) Å, c = 8.9308(6) Å, α = 90°, β = 98.074(3)°, γ = 90°, V = 2217.8(3) Å^3; Z = 4, ρ_{calcd} = 1.428 g cm^{-3}; crystal dimensions 0.200 × 0.150 × 0.050 mm^3; θ_{max} = 33.129°; 68772 reflections, 7415 independent (R_{int} = 0.0419), intrinsic phasing; absorption coeff (μ = 1.014 mm^{-1}), absorption correction semiempirical from equivalents (SADABS);

https://dx.doi.org/10.1021/acs.organomet.0c00161
Organometallics XXXX, XXX, XXX−XXX

refinement (against F_o^2) with SHELXTL V6.1, 286 parameters, 0 restraints, R_1 = 0.0453 ($I > 2\sigma$) and wR_2 = 0.0915 (all data), GoF = 1.054, residual electron density 0.647/−0.642 e Å^{-3}.

Crystal Structure Data for ***6*** *(CCDC No. 1985567).* X-ray quality crystals were grown following diffusion of diethyl ether vapor into a $CHCl_3$ solution of the compound at room temperature. Crystal structure parameters: $C_{19}H_{20}Cl_1N_3Ni_1$ 384.54 g/mol, triclinic, space group $P\bar{1}$; a = 9.8825(13) Å, b = 14.352(3) Å, c = 24.736(4) Å, α = 90.844(12)°, β = 94.338(10)°, γ = 102.995(13)°, V = 3406.9(10) Å^3; Z = 8, ρ_{calcd} = 1.499 g cm^{-3}; crystal dimensions 0.300 × 0.200 × 0.050 mm^3; θ_{max} = 30.679°; 97358 reflections, 20976 independent (R_{int} = 0.1012), intrinsic phasing; absorption coeff (μ = 1.300 mm^{-1}), absorption correction semiempirical from equivalents (SADABS); refinement (against F_o^2) with SHELXTL V6.1, 881 parameters, 0 restraints, R_1 = 0.0601 ($I > 2\sigma$) and wR_2 = 0.1253 (all data), GoF = 1.021, residual electron density 0.770/−0.722 e Å^{-3}.

Representative Procedure for Catalytic Trials. To a 50 mL Teflon stoppered flask catalyst **4c** (0.012 g, 0.05 mmol), LiO*t*Bu (0.081 g, 1.01 mmol), benzoxazole (**H2**; 0.12 g, 1.01 mmol), and 1-iodooctane (**A1**; 0.291 g, 0.75 mmol), added 1,4-dioxane (2.0 mL) inside an N_2-filled glovebox. The resulting reaction mixture was stirred in a preheated oil bath set to 140 °C for 16 h. An aliquot (10 μL) of the reaction mixture diluted with 1 mL acetone was injected to GC instrument to analyze the products. GC yields of the products were obtained from the calibration curves plotted for pure reactants and products, with biphenyl as an internal standard, and are reported as an average of two runs.

■ ASSOCIATED CONTENT

Supporting Information

The Supporting Information is available free of charge at https://pubs.acs.org/doi/10.1021/acs.organomet.0c00161.

Extended experimental details (preparation of precursors, GC method details, additive experiments) and full characterization data (multinuclear NMR spectra and HR-MS spectra of all new compounds) (PDF)

Accession Codes

CCDC 1985563−1985568 contain the supplementary crystallographic data for this paper. These data can be obtained free of charge via www.ccdc.cam.ac.uk/data_request/cif, or by emailing data_request@ccdc.cam.ac.uk, or by contacting The Cambridge Crystallographic Data Centre, 12 Union Road, Cambridge CB2 1EZ, UK; fax: +44 1223 336033.

■ AUTHOR INFORMATION

Corresponding Author

David E. Herbert − *Department of Chemistry and the Manitoba Institute of Materials, University of Manitoba, Winnipeg, Manitoba R3T 2N2, Canada;* orcid.org/0000-0001-8190-2468; Email: david.herbert@umanitoba.ca

Authors

Pavan Mandapati − *Department of Chemistry and the Manitoba Institute of Materials, University of Manitoba, Winnipeg, Manitoba R3T 2N2, Canada;* orcid.org/0000-0002-3686-4850

Jason D. Braun − *Department of Chemistry and the Manitoba Institute of Materials, University of Manitoba, Winnipeg, Manitoba R3T 2N2, Canada;* orcid.org/0000-0002-5850-8048

Baldeep K. Sidhu − *Department of Chemistry and the Manitoba Institute of Materials, University of Manitoba, Winnipeg, Manitoba R3T 2N2, Canada;* orcid.org/0000-0002-2016-6601

Gabrielle Wilson − *Department of Chemistry and the Manitoba Institute of Materials, University of Manitoba, Winnipeg, Manitoba R3T 2N2, Canada*

Complete contact information is available at: https://pubs.acs.org/10.1021/acs.organomet.0c00161

Notes

The authors declare no competing financial interest.

■ ACKNOWLEDGMENTS

The following sources of funding are gratefully acknowledged: Natural Sciences Engineering Research Council of Canada for a USRA (GW) and a Discovery Grant to DEH (RGPIN-2014-03733); the Canadian Foundation for Innovation and Research Manitoba for an award in support of an X-ray diffractometer (CFI #32146); and the University of Manitoba for GETS support (PM, JDB). We are also grateful to Bin Huang for assistance collecting spectra of **2c**.

■ REFERENCES

(1) Kulkarni, A. A.; Daugulis, O. Direct Conversion of Carbon-Hydrogen Into Carbon-Carbon Bonds by First-Row Transition Metal Catalysis. *Synthesis* **2009**, 4087−4109.

(2) Ackermann, L. Metal-Catalyzed Direct Alkylations of (Hetero)-arenes via C-H Bond Cleavages With Unactivated Alkyl Halides. *Chem. Commun.* **2010**, *46*, 4866−4877.

(3) Ping, L.; Chung, D. S.; Bouffard, J.; Lee, S.-G. Transition Metal-Catalyzed Site- and Regio-Divergent C-H Bond Functionalization. *Chem. Soc. Rev.* **2017**, *46*, 4299−4328.

(4) Qin, Y.; Zhu, L.; Luo, S. Organocatalysis in Inert C-H Bond Functionalization. *Chem. Rev.* **2017**, *117*, 9433−9520.

(5) Hu, X. Nickel-Catalyzed Cross Coupling of Non-Activated Alkyl Halides: a Mechanistic Perspective. *Chem. Sci.* **2011**, *2*, 1867−1886.

(6) Verrier, C.; Hoarau, C.; Marsais, F. Direct Palladium-Catalyzed Alkenylation, Benzylation and Alkylation of Ethyl Oxazole-4-Carboxylate with Alkenyl-, Benzyl- and Alkyl Halides. *Org. Biomol. Chem.* **2009**, *7*, 647−650.

(7) Yao, T.; Hirano, K.; Satoh, T.; Miura, M. Palladium- and Nickel-Catalyzed Direct Alkylation of Azoles with Unactivated Alkyl Bromides and Chlorides. *Chem. - Eur. J.* **2010**, *16*, 12307−12311.

(8) Vechorkin, O.; Proust, V.; Hu, X. The Nickel/Copper-Catalyzed Direct Alkylation of Heterocyclic C-H Bonds. *Angew. Chem., Int. Ed.* **2010**, *49*, 3061−3064.

(9) Ackermann, L.; Punji, B.; Song, W. User-Friendly [(Diglyme)-$NiBr_2$]-Catalyzed Direct Alkylations of Heteroarenes with Unactivated Alkyl Halides through C-H Bond Cleavages. *Adv. Synth. Catal.* **2011**, *353*, 3325−3329.

(10) Patel, U. N.; Pandey, D. K.; Gonnade, R. G.; Punji, B. Synthesis of Quinoline-Based NNN-Pincer Nickel(II) Complexes: A Robust and Improved Catalyst System for C-H Bond Alkylation of Azoles With Alkyl Halides. *Organometallics* **2016**, *35*, 1785−1793.

(11) Yao, T.; Hirano, K.; Satoh, T.; Miura, M. Nickel- and Cobalt-Catalyzed Direct Alkylation of Azoles with N-Tosylhydrazones Bearing Unactivated Alkyl Groups. *Angew. Chem., Int. Ed.* **2012**, *51*, 775−779.

(12) Theunissen, C.; Wang, J.; Evano, G. Copper-Catalyzed Direct Alkylation of Heteroarenes. *Chem. Sci.* **2017**, *8*, 3465−3470.

(13) Zhao, X.; Wu, G.; Zhang, Y.; Wang, J. Copper-Catalyzed Direct Benzylation or Allylation of 1,3-Azoles with N-Tosylhydrazones. *J. Am. Chem. Soc.* **2011**, *133*, 3296−3299.

(14) Ren, P.; Salihu, I.; Scopelliti, R.; Hu, X. Copper-Catalyzed Alkylation of Benzoxazoles with Secondary Alkyl Halides. *Org. Lett.* **2012**, *14*, 1748−1751.

(15) Mandapati, P.; Giesbrecht, P. K.; Davis, R. L.; Herbert, D. E. Phenanthridine-Containing Pincer-like Amido Complexes of Nickel, Palladium, and Platinum. *Inorg. Chem.* **2017**, *56*, 3674−3685.

(16) Mondal, R.; Giesbrecht, P. K.; Herbert, D. E. Nickel(II), Copper(I) and Zinc(II) Complexes Supported by a (4-Diphenylphosphino)phenanthridine Ligand. *Polyhedron* **2016**, *108*, 156−162.
(17) Nainwal, L. M.; Tasneem, S.; Akhtar, W.; Verma, G.; Khan, M. F.; Parvez, S.; Shaquiquzzaman, M.; Akhter, M.; Alam, M. M. Green Recipes to Quinoline: A Review. *Eur. J. Med. Chem.* **2019**, *164*, 121−170.
(18) Braun, J. D.; Lozada, I. B.; Kolodziej, C.; Burda, C.; Newman, K. M. E.; van Lierop, J.; Davis, R. L.; Herbert, D. E. Iron(II) Coordination Complexes With Panchromatic Absorption and Nanosecond Charge-Transfer Excited State Lifetimes. *Nat. Chem.* **2019**, *11*, 1144−1150.
(19) Gunanathan, C.; Gnanaprakasam, B.; Iron, M. A.; Shimon, L. J. W.; Milstein, D. Long-Range" Metal-Ligand Cooperation in H_2 Activation and Ammonia-Promoted Hydride Transfer with a Ruthenium-Acridine Pincer Complex. *J. Am. Chem. Soc.* **2010**, *132*, 14763−14765.
(20) Patel, U. N.; Jain, S.; Pandey, D. K.; Gonnade, R. G.; Vanka, K.; Punji, B. Mechanistic Aspects of Pincer Nickel(II)-Catalyzed C-H Bond Alkylation of Azoles with Alkyl Halides. *Organometallics* **2018**, *37*, 1017−1025.
(21) Lozada, I. B.; Murray, T.; Herbert, D. E. Monomeric Zinc(II) Amide Complexes Supported by Bidentate, Benzannulated Phenanthridine Amido Ligands. *Polyhedron* **2019**, *161*, 261−267.
(22) Mandapati, P.; Braun, J. D.; Killeen, C.; Davis, R. L.; Williams, J. A. G.; Herbert, D. E. Luminescent Platinum(II) Complexes of *N^N⁻^N* Amido Ligands with Benzannulated N-Heterocyclic Donor Arms: Quinolines Offer Unexpectedly Deeper Red Phosphorescence than Phenanthridines. *Inorg. Chem.* **2019**, *58*, 14808−14817.
(23) Giesbrecht, P. K.; Nemez, D. B.; Herbert, D. E. Electrochemical Hydrogenation of a Benzannulated Pyridine to a Dihydropyridine in Acidic Solution. *Chem. Commun.* **2018**, *54*, 338−341.
(24) Mondal, R.; Lozada, I. B.; Davis, R. L.; Williams, J. A. G.; Herbert, D. E. Site-Selective Benzannulation of N-Heterocycles in Bidentate Ligands Leads to Blue-Shifted Emission from $[(P\text{^}N)\text{-}Cu]_2(\mu\text{-}X)_2$ Dimers. *Inorg. Chem.* **2018**, *57*, 4966−4978.
(25) Csok, Z.; Vechorkin, O.; Harkins, S. B.; Scopelliti, R.; Hu, X. Nickel Complexes of a Pincer NN_2 Ligand: Multiple Carbon-Chloride Activation of CH_2Cl_2 and $CHCl_3$ Leads to Selective Carbon-Carbon Bond Formation. *J. Am. Chem. Soc.* **2008**, *130*, 8156−8157.
(26) Omer, H. M.; Liu, P. Computational Study of Ni-Catalyzed C-H Functionalization: Factors That Control the Competition of Oxidative Addition and Radical Pathways. *J. Am. Chem. Soc.* **2017**, *139*, 9909−9920.
(27) Hill, R. H.; Puddephatt, R. J. A Mechanistic Study of the Photochemically Initiated Oxidative Addition of Isopropyl Iodide to Dimethyl(1,10-phenanthroline)platinum(II). *J. Am. Chem. Soc.* **1985**, *107*, 1218−1225.
(28) Torigoe, T.; Ohmura, T.; Suginome, M. Asymmetric Cycloisomerization of o-Alkenyl-N-Methylanilines to Indolines by Iridium-Catalyzed $C(sp^3)$-H Addition to Carbon-Carbon Double Bonds. *Angew. Chem., Int. Ed.* **2017**, *56*, 14272−14276.
(29) Medina Padilla, M.; Castro Morera, A.; Sanchez-Quesada, J.; Garcia Palomero, E.; Alonso Cascon, M.; Herrero Santos, S.; Vela Ruiz, M.; Usan Egea, P.; Rodriguez Villanueva, A. L. Triple Substituted Phenanthroline Derivatives for the Treatment of Neurodegenerative or Haematological Diseases or Conditions, or Cancer. Patent Number: US20110306631A12011.
(30) Koradin, C.; Dohle, W.; Rodriguez, A. L.; Schmid, B.; Knochel, P. Synthesis of Polyfunctional Indoles and Related Heterocycles Mediated by Cesium and Potassium Bases. *Tetrahedron* **2003**, *59*, 1571−1587.
(31) *APEX3* v2016.1−0; Bruker-AXS: Madison, WI, 2016.
(32) Sheldrick, G. M. A Short History of SHELX. *Acta Crystallogr., Sect. A: Found. Crystallogr.* **2008**, *A64*, 112−122.
(33) Spek, A. L. Structure Validation in Chemical Crystallography. *Acta Crystallogr., Sect. D: Biol. Crystallogr.* **2009**, *D65*, 148−155.

https://dx.doi.org/10.1021/acs.organomet.0c00161
Organometallics XXXX, XXX, XXX−XXX